Remote Sensing in Ecology and Conservation
Open Access
ZSL LET'S WORK FOR WILDLIFE

RESEARCH ARTICLE

Radar and multispectral remote sensing data accurately estimate vegetation vertical structure diversity as a fire resilience indicator

José Manuel Fernández-Guisuraga[1], Susana Suárez-Seoane[2] & Leonor Calvo[1]

[1]Area of Ecology, Department of Biodiversity and Environmental Management, Faculty of Biological and Environmental Sciences, University of León, 24071, León, Spain
[2]Department of Organisms and Systems Biology (Ecology Unit) and Research Institute of Biodiversity (IMIB; UO-CSIC-PA), University of Oviedo, Oviedo, Mieres, Spain

Keywords
Fire, resilience, SAR, Sentinel, vertical structure diversity

Correspondence
José Manuel Fernández-Guisuraga, Area of Ecology, Department of Biodiversity and Environmental Management, Faculty of Biological and Environmental Sciences, University of León, 24071 León, Spain.
Tel: +34 987291520; E-mail: jofeg@unileon.es

Funding Information
This study was financially supported by the Spanish Ministry of Economy and Competitiveness, and the European Regional Development Fund (ERDF), in the framework of the FIRESEVES (AGL2017-86075-C2-1-R) project; by the Regional Government of Castilla and León in the framework of the WUIFIRECYL (LE005P20) project; and by the British Ecological Society in the framework of the SR22-100154 project, where José Manuel Fernández-Guisuraga is the Principal Investigator.

Editor: Mat Disney
Associate Editor: Wang Li

Received: 22 April 2022; Revised: 21 June 2022; Accepted: 29 July 2022

Abstract

The structural complexity of plant communities contributes to maintaining the ecosystem functioning in fire-prone landscapes and plays a crucial role in driving ecological resilience to fire. The objective of this study was to evaluate the resilience to fire off several plant communities with reference to the temporal evolution of their vertical structural diversity (VSD) estimated from the data fusion of C-band synthetic aperture radar (SAR) backscatter (Sentinel-1) and multispectral remote sensing reflectance (Sentinel-2) in a burned landscape of the western Mediterranean Basin. We estimated VSD in the field 1 and 2 years after fire using Shannon's index as a measure of vertical heterogeneity in vegetation structure from the vegetation cover in several strata, both in burned and unburned control plots. Random forest (RF) was used to model VSD in the control (analogous to prefire scenario) and burned plots (1 year after fire) using as predictors (i) Sentinel-1 VV and VH backscatter coefficients and (ii) surface reflectance of Sentinel-2 bands. The transferability of the RF model from 1 to 2 years after wildfire was also evaluated. We generated VSD prediction maps across the study site for the prefire scenario and 1 to 4 years postfire. RF models accurately explained VSD in unburned control plots (R^2 = 87.68; RMSE = 0.16) and burned plots 1 year after fire (R^2 = 80.48; RMSE = 0.13). RF model transferability only involved a reduction in the VSD predictive capacity from 0.13 to 0.20 in terms of RMSE. The VSD of each plant community 4 years after the fire disturbance was significantly lower than in the prefire scenario. Plant communities dominated by resprouter species featured significantly higher VSD recovery values than communities dominated by facultative or obligate seeders. Our results support the applicability of SAR and multispectral data fusion for monitoring VSD as a generalizable resilience indicator in fire-prone landscapes.

doi: 10.1002/rse2.299

Introduction

Wildfires are a key ecosystem process in the western Mediterranean Basin (González-De Vega et al., 2016; Pausas et al., 2008) that sharply determines the dynamics in the composition and structure of plant communities (Calvo et al., 2008; Doblas-Miranda et al., 2017; Fernández-Guisuraga, Suárez-Seoane, et al., 2019). In this region, the resilience of plant communities under historical fire disturbance regimes supports the recovery to prefire levels of their structure and composition (Johnstone et al., 2016; Seidl et al., 2014). However, the observed and projected increase

in the frequency and severity of wildfires (San-Miguel-Ayanz et al., 2012), as a consequence of current aridity levels (Vieira et al., 2010) and rural land abandonment (Sagra et al., 2019), may jeopardize vegetation resilience to fire (Doblas-Miranda et al., 2017). In this sense, recurrent and severe wildfires can exert strong effects on regenerative strategies (i.e., resprouting and seeding capacity) that may impair plant community recovery (Johnstone et al., 2016; Meng et al., 2018; Zhao et al., 2016).

Among the components that drive forest ecological resilience to fire, defined as the ecosystem capacity to absorb disturbance before switching to an alternate stable state (Folke, 2006; Gunderson & Holling, 2002; Müller et al., 2016; Newton & Cantarello, 2015), the structural complexity of plant communities plays a crucial role (Chergui et al., 2018). Forest vertical structural complexity can assist in maintaining the ecosystem functioning and processes of fire-prone landscapes (Drever et al., 2006; González-De Vega et al., 2016) for its connections with the (i) diversity of plant functional traits related to the physical arrangement of vegetation in the vertical profile (Gara et al., 2018; LaRue et al., 2019), (ii) primary production (Gough et al., 2019), and (iii) soil nutrient availability (LaRue et al., 2019). In addition, the heterogeneity in vertical vegetation structure is heavily linked with physical niche space and wildlife habitat (Wood et al., 2012). Therefore, the assessment of how the structural complexity of plant communities recovers to a pre-disturbance state is essential for improving the knowledge about ecological resilience in fire-prone ecosystems (González-De Vega et al., 2016) and providing new insights into the implementation of postfire management actions (Fernández-Guisuraga et al., 2020).

Several metrics of forest vertical structure diversity from field-based inventories have been proposed in the literature such as the foliage-height diversity index (FHD; MacArthur & MacArthur, 1961), variation of plant height (Wiens & Rotenberry, 1981) or diameter at breast height (Montes et al., 2005), cover by plant life forms (Williams & Marsh, 1998), habitat heterogeneity index (HH; Freemark & Merriam, 1986) or stand structural index (STVI; Staudhammer & LeMay, 2001). Among these metrics, FHD or slight modifications of this index are the most commonly used in Mediterranean ecosystems to quantify vertical heterogeneity in vegetation structure due to its flexibility and straightforward application (Wood et al., 2012). For instance, Meeussen et al. (2020) examined the variation in forest edge structural metrics, including FHD, in sub-Mediterranean biomes across Europe. FHD metric was also used to explore the long-term effects of fuel reduction treatments on understory vegetation in Mediterranean forests in southern Portugal (Santana et al., 2011). Suárez-Seoane et al. (2002) assessed the effects of agricultural abandonment on FHD across a successional gradient in a Mediterranean region in northwest Spain. However, field-based inventories of vertical structure diversity are labor-intensive and time-consuming for monitoring large areas, especially in time-series analyses (Fernández-Guisuraga, Suárez-Seoane, & Calvo, 2021), and do not allow spatially explicit (i.e., wall-to-wall) measurements (Bergen et al., 2009). Hence, approaches based exclusively on field data present little versatility for resilience assessments in large burned areas. In this sense, remote sensing earth observations offer nowadays an efficient way to accomplish this objective (Fernández-Guisuraga et al., 2020).

Most research on forest resilience quantification using remote sensing techniques has been based to date on the monitorization of vegetation greenness recovery through vegetation spectral indices (VIs) computed from passive optical data (e.g., Cuevas-González et al., 2009; Ireland & Petropoulos, 2015; Jin et al., 2012; Vila & Barbosa, 2010). The drawback of this approach in burned areas is related to the (i) lack of physical sense because VIs are not intrinsic physical quantities (Fernández-Guisuraga, Suárez-Seoane, & Calvo, 2021), (ii) performance loss attributable to the background signal of charred material and soil in recently burned areas (Vila & Barbosa, 2010), (iii) canopy variability regarding vegetation greenness while exhibiting identical biophysical properties (Veraverbeke et al., 2012), and (iv) reflectance signal saturation at high vegetation cover (Lu et al., 2016). Other remote sensing approaches have used the fractional vegetation cover (FVC) retrieved from time series of passive optical satellite data as a resilience indicator using pixel unmixing models (Fernández-Guisuraga et al., 2020; Fernandez-Manso et al., 2016) and radiative transfer models (Fernández-Guisuraga, Suárez-Seoane, & Calvo, 2021). However, such a resilience indicator exclusively reflects the recovery of the green vegetation fraction at the top of canopy when dealing with passive remote sensing data and plant communities that feature several strata (Fernández-Guisuraga, Suárez-Seoane, & Calvo, 2021). Conversely, active remote sensors, such as light detection and ranging (LiDAR) and synthetic aperture radar (SAR), enable the characterization of vegetation structural and biophysical properties in the vertical profile (Bergen et al., 2009; Fernández-Guisuraga, Suárez-Seoane, et al., 2022) because of their sensitivity to the quantity and distribution of scatterers in the canopy (Tanase et al., 2015). Unfortunately, the limited temporal availability of LiDAR data prevents the analysis of postfire recovery trajectories in forest resilience assessments (Wood et al., 2012). Despite the potential, physical sense, and unlimited availability of SAR backscatter data in the characterization of vegetation vertical structure in burned landscapes (Kalogirou et al., 2014), to date this approach remains

completely unexplored for quantifying vertical structural diversity in burned areas, and particularly, for estimating this parameter as a resilience indicator in fire-prone ecosystems.

Remarkably, SAR acquisitions are independent of cloud cover and sun illumination (Belenguer-Plomer et al., 2019), and the signal penetrates and interacts with the vegetation canopy components in a magnitude that depends on the SAR wavelength (Jagdhuber, 2012) but also on canopy closure and architecture (Bartsch et al., 2020; Inoue et al., 2002). Specifically, shorter SAR wavelengths (e.g., C-band) are sensitive to canopy leaves and small branches and feature a lower penetration into the canopy than longer wavelengths (e.g., L band) (Patenaude et al., 2005). For that reason, the estimation of vegetation structural parameters through C-band SAR data is deemed appropriate for regions with low to moderate vegetation standing biomass and canopy closure (Lu et al., 2016; Patenaude et al., 2005). However, in this scenario, increased ground scattering and soil moisture effect on SAR signal must be considered in SAR time-series acquisitions (Minchella et al., 2009).

The synergistic use of SAR backscatter and passive optical reflectance data can also provide integrated insights into the vertical stand structure and the vegetation biophysical parameters since optical data are sensitive to vegetation type, architecture, and traits of the uppermost section of the canopy (Healey et al., 2020; Montesano et al., 2013), which are also strongly related to the stand structural complexity (Conti et al., 2021). Thus, the fusion of optical and SAR data would provide complementary information on the vegetation vertical structure (Lu et al., 2016) and reduce the soil background influence on the retrieval of structural parameters compared with the individual use of SAR images (Wang et al., 2019). This approach has been shown to improve the estimation of structural parameters such as leaf area index or aboveground biomass worldwide (e.g., Huang et al., 2016; Montesano et al., 2013; Naidoo et al., 2019), but, as with SAR data alone, there are no studies up to date that exploit this approach for mapping vertical structural diversity and vegetation resilience in burned areas.

The objective of this study was to evaluate the resilience to fire off several plant communities with reference to the temporal evolution of their vertical structural diversity estimated from the fusion of C-band SAR backscatter (Sentinel-1) and multispectral (Sentinel-2) remote sensing data. Specifically, we selected as case study a burned landscape of the western Mediterranean Basin that comprises several plant communities dominated by either shrub or tree species. Vertical structure diversity index was measured in each community using Shannon's index applied to vegetation cover data in several strata and modeled across the pre and postfire time series using Sentinel-1 and Sentinel-2.

Materials and Methods

The methodology comprised the following three steps (Fig. 1): field data acquisition, remote sensing data acquisition/processing, and data analysis.

Study site

The study site is located in the northwestern Iberian Peninsula within the Sierra de Cabrera mountain range, where a wildfire that occurred between 21 and 27 August 2017 and burned 9940 ha of forest and shrubland plant communities (Fig. 2). The site is characterized by rugged topography with altitudes ranging between 836 and 1938 m above sea level and is dominated by siliceous lithologies, mainly slates and quartzites (GEODE, 2022). The region lies in a transition area between Mediterranean and Eurosiberian biogeographic conditions (Rivas-Martínez et al., 2011). Annual mean precipitation in the study site ranges between 600 and 1500 mm and annual mean temperature between 5°C and 15°C for a 50-year period (Ninyerola et al., 2005), corresponding to a Mediterranean temperate climate (García-Llamas et al., 2019). Extreme fire weather conditions regarding maximum temperatures and relative humidity were recorded during the fire progression (García-Llamas et al., 2020).

The wildfire affected gorse *Genista hystrix* Lange and broom *Genista florida* L. shrublands dominated by facultative seeders, as well as heath *Erica australis* L. shrublands dominated by resprouter species. The wildfire also affected forests dominated by the resprouter Pyrenean oak *Quercus pyrenaica* Willd. and the obligate seeder Scots pine *Pinus sylvestris* L. The plant communities were mapped (Fig. 2) using a prefire Sentinel-2 multispectral image classified by means of the maximum likelihood algorithm (Strahler, 1980), with an overall accuracy of 91%. See Fernández-Guisuraga, Suárez-Seoane, García-Llamas, et al. (2021) for more details on the computation of the vegetation classification map.

Field data

One year after the wildfire event (June 2018), 74 field plots of 30 × 30 m were established in relatively homogeneous areas regarding vegetation legacies within the fire perimeter (Fig. 2) for calibrating and validating remote sensing retrievals in postfire scenarios. Following an unburned control plot approach (Díaz-Delgado et al., 2002), 40 additional field plots of 30 × 30 m were located in unburned areas for assessing prefire retrievals. Burned

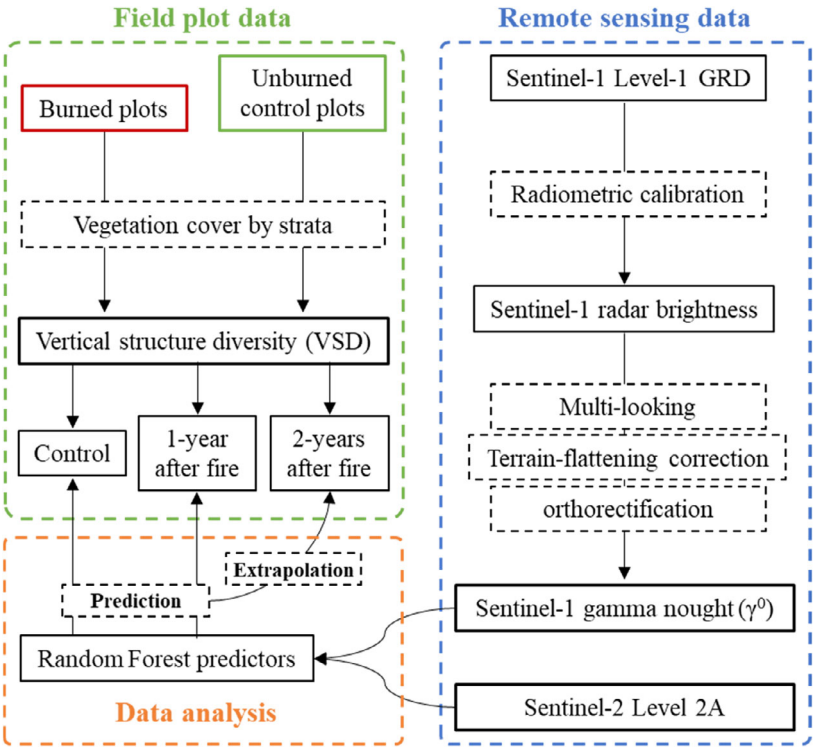

Figure 1. Methodology workflow of the present study.

and control plots were equally stratified into the plant communities of the study site, ensuring a minimum separation of 200 m between plots. The plots were located in the field using a submeter accuracy GPS receiver and were initially surveyed in June 2018 (both burned and control plots) as well as in June 2019 (burned plots). Within each plot, we established a group of four subplots of 2 × 2 m at azimuths of 45°, 135°, 225°, and 315°, located 6.5 m away from the plot center (Fernández-Guisuraga, Calvo, et al., 2022). Within the subplots, we estimated vegetation cover as the vertical projected area occupied by vegetation in several strata (0–0.5, 0.5–1, 1–4, and >4 m) corresponding to the herbaceous, low shrub, tall shrub, and overstory layers (Casenave et al., 1995), using a visual estimation method in steps of 5% (Delamater et al., 2012) following the protocol of Fernández-Guisuraga, Verrelst, et al. (2021). Depending on the height stratum, vegetation cover was estimated in a top-down or bottom-up direction using a quadrat and long sticks as estimation assistance (Fernández-Guisuraga, Suárez-Seoane, & Calvo, 2021; Fernández-Guisuraga, Verrelst, et al., 2021). The vegetation cover per stratum for each plot of 30 × 30 m was obtained by averaging the estimation of the four subplots of 2 × 2 m. Vertical structure diversity index (VSD) was calculated for each plot using Shannon's index (unitless), analogous to the calculation of FHD (MacArthur & MacArthur, 1961) but using an appropriate notation to the present methodology (foliage vs. cover; Angelo, 2010):

$$\mathrm{VSD} = -\sum_{i=1}^{S} p_i \ln p_i,$$

where p_i is the proportion of vegetation cover in the ith stratum, and S is the total number of strata.

Remote sensing data sources and processing

Sentinel-1

The Sentinel-1 mission of the Copernicus program of the European Space Agency (ESA) comprises a constellation of two C-band (wavelength of 5.6 cm) SAR polar-orbiting satellites launched in April 2014 (Sentinel-1A) and April 2016 (Sentinel-1B). This constellation provides a 6-days repeat cycle at the equator and operates in four imaging acquisition modes with different spatial resolution and coverage (ESA, 2022a). Five Sentinel-1 SAR scenes were acquired from the Copernicus Open Access Hub (https://scihub.copernicus.eu/) during peak biomass of the study site in the summer months between 2017 and 2021 (Table 1), as close as possible to the end dates of the field sampling campaigns of summer 2018 and 2019. We also avoided SAR scene acquisitions in which precipitation

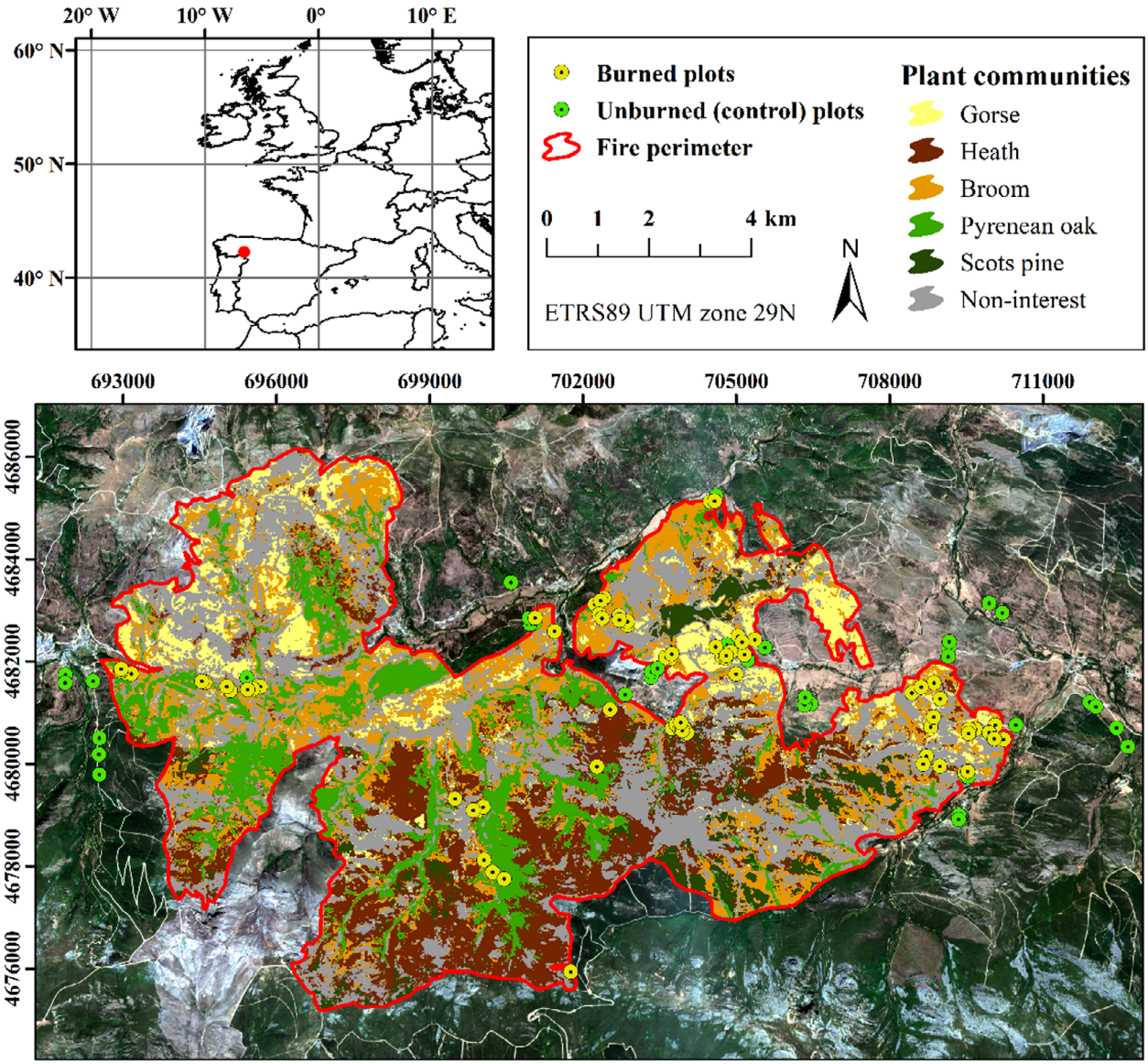

Figure 2. Study site within the perimeter of Sierra de Cabrera wildfire (9940 ha), plant community classification map (Fernández-Guisuraga, Suárez-Seoane, García-Llamas, et al., 2021), and location of the burned and control plots.

events have been recorded for 7 days prior to the SAR image date (AEMET, 2022) due to the influence of soil moisture on SAR backscatter (Belenguer-Plomer et al., 2019). SAR scenes were a Level-1 Ground Range Detected (GRD) product acquired in interferometric wide swath mode at dual polarization (VV vertical-vertical + VH vertical-horizontal) (ESA, 2022b). GRD products were preprocessed using the Sentinel-1 Toolbox (S1TBX; ESA, 2022c). The processing chain included (i) radiometric calibration to radar brightness, (ii) multi-looking to the nominal Sentinel-1 resolution (20 m square pixels), (iii) terrain-flattening correction (Small, 2011) for removing topographic effects, and (iv) orthorectification using the range Doppler method (Small & Schubert, 2008). Finally, gamma naught (γ^0) backscatter coefficients of VV and VH polarizations were log-transformed to dB units. γ^0 VV and VH values of the year 2018 and 2019 scenes were extracted for each field plot of 30 × 30 m by averaging the values of a regular grid of points (spacing of 5 m) systematically sampled (Picotte & Robertson, 2011) due to the overlap of several pixels within each plot.

Sentinel-2

Sentinel-2 is a multispectral satellite mission also included in the ESA Copernicus program. The mission comprises

Table 1. Acquisition date of Sentinel-1 and Sentinel-2 scenes.

	Satellite	Acquisition date	Time since fire
Sentinel-1 scene #			
1	1A	7 August 2017 18:19:36 UTC	Prefire (14 days)
2	1A	21 July 2018 18:19:41 UTC	1 year
3	1A	28 July 2019 18:19:48 UTC	2 years
4	1A	10 July 2020 18:19:53 UTC	3 years
5	1A	29 July 2021 18:20:00 UTC	4 years
Sentinel-2 scene #			
1	2A	13 August 2017 11:21:21 UTC	Prefire (7 days)
2	2A	29 July 2018 11:21:11 UTC	1 year
3	2B	29 June 2019 11:21:19 UTC	2 years
4	2A	18 July 2020 11:21:21 UTC	3 years
5	2B	17 August 2021 11:21:19 UTC	4 years

two polar-orbiting satellites launched in June 2015 (Sentinel-2A) and March 2017 (Sentinel-2B), which feature a revisit time of 5 days at the equator. Sentinel-2 MultiSpectral Instrument (MSI) on-board satellite platforms is a push-broom sensor that provides 13 spectral bands over the visible (VIS), near-infrared (NIR), and shortwave infrared (SWIR) regions of the electromagnetic spectrum at different spatial resolutions (ESA, 2022d) (Table 2).

Sentinel-2 MSI Level 2A scenes covering the study site were also obtained from the Copernicus Open Access Hub. Specific acquisition dates (Table 1) were chosen on the basis of the availability of cloud-free scenes closest to field campaigns and Sentinel-1 scene dates. Level 2A is a surface reflectance product corrected for topographic and atmospheric effects by the image provider (ESA, 2022d). The nearest neighbor resampling technique was used to downsample bands at 10 m of spatial resolution to 20 m. We discarded the bands at 60 m because they are heavily affected by atmospheric effects (Jia et al., 2016). Sentinel-2 surface reflectance values for the year 2018 and 2019 scenes were extracted for each plot of 30 × 30 m following the same procedure as for Sentinel-1 backscatter data.

Data analysis

Random Forest (RF) regression (Breiman, 2001) ensemble learning algorithm was used to model VSD in the control (analogous to prefire scenario) and burned plots (1 year after fire) using as predictors (i) Sentinel-1 VV and VH backscatter coefficients and (ii) surface reflectance of Sentinel-2 bands. RF can properly handle spatial autocorrelation in the predictors (García-Llamas et al., 2020) and minimize overfitting issues (Cutler et al., 2007). The increase in mean square error (%IncMSE) and the internal out-of-bag error rate parameters were used to assess the relative importance of the predictors and the variance explained (pseudo-R^2) by the model, respectively. RF models were calibrated with the *randomForest* function using the *RandomForest* package (Liaw & Wiener, 2002) in R 4.0.5 (R Core Team, 2021). Model parameter *mtry* was tuned using the *trainControl* and *train* functions (Fernández-García et al., 2022) of *caret* package (Kuhn, 2020), whereas *ntree* parameter was set to 1000, which balances stable model predictions with computational efficiency (Probst & Boulesteix, 2018). A parsimonious subset of predictors that maximize model robustness and VSD prediction performance was selected through recursive feature elimination based on five times repeated 10-fold cross-validation using *rfeControl* and *rfe* functions (Fernández-García et al., 2022) within *caret* package. The univariate relationships between VSD and remote sensing predictors were examined through scatterplots.

RF model object of the burned plots (1 year after fire) was used to generate VSD predictions for 2019 (2 years after fire) with contemporaneous Sentinel-1 and Sentinel-2 data. The coefficient of determination (R^2) and the root mean-squared error (RMSE) were computed to quantify prediction performance. Burned and control RF model objects were used to generate VSD prediction maps across the study site for the prefire scenario and 1–4 years post-fire using *raster* (Hijmans, 2021) and *rgdal* (Bivand et al., 2021) packages. Although we calibrated and validated RF models in the prefire scenario, as well as 1 and 2 years after fire, we generated predictions beyond that time period to analyze the evolution of the VSD in the longer term, similar to previous remote sensing research (e.g., Fernández-Guisuraga et al., 2020). A random sampling of 10 000 points stratified by plant community was performed within the fire perimeter to extract VSD values for each period of the time series. A minimum distance of 100 m between points was ensured. A one-way

Table 2. Sentinel-2A band configuration.

Sentinel-2 band #	B1	B2	B3	B4	B5	B6	B7	B8	B8A	B9	B10	B11	B12
Spatial resolution (m)	60	10	10	10	20	20	20	10	20	60	60	20	20
Region	VIS	VIS	VIS	VIS	NIR	NIR	NIR	NIR	NIR	NIR	SWIR	SWIR	SWIR
Band center (nm)	443	492	560	665	704	741	783	833	865	945	1374	1614	2202
Bandwidth (nm)	21	66	36	31	15	15	20	106	21	20	31	91	175

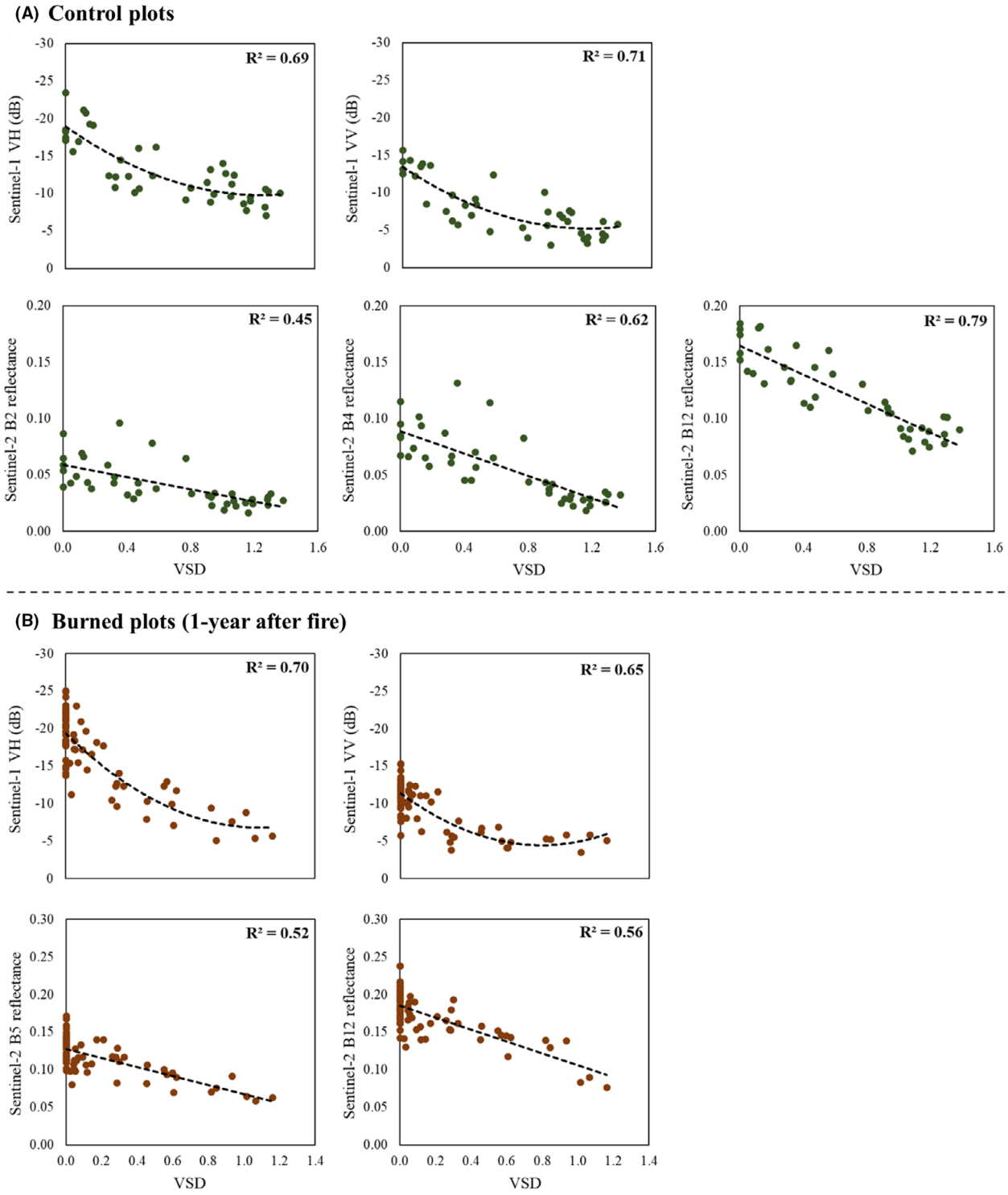

Figure 3. Relationship between Sentinel-1 and Sentinel-2 predictors included in Random Forest (RF) parsimonious models and vertical structure diversity index (VSD) in unburned control plots (A) and burned plots 1 year after fire (B).

repeated measures ANOVA (1w-rmANOVA) and subsequent Tukey's HSD test were performed in *rstatix* (Kassambara, 2021) package to determine the earliest point in the postfire time series where VSD values for each plant community do not differ significantly from prefire VSD. The VSD recovery (%) for each plant community was

computed as the ratio of 4 years postfire to prefire VSD estimates. A one-way ANOVA (1w-ANOVA) and subsequent Tukey's HSD test were implemented to evaluate VSD recovery differences as a function of the plant community. Statistical significance was determined at the 0.05 level.

Results

The fusion of Sentinel-1 backscatter coefficients and Sentinel-2 surface reflectance data accurately explained VSD in unburned control plots (R^2 = 87.68; RMSE = 0.16) and burned plots 1 year after fire (R^2 = 80.48; RMSE = 0.13) through parsimonious RF models. The relationships between Sentinel-1 predictors and VSD were quadratic and direct, whereas Sentinel-2 predictors featured a linear and inverse relationship with VSD (Fig. 3). In the burned plots, Sentinel-1 backscatter coefficients showed a stronger correlation with VSD (R^2 = 0.65–0.70) than Sentinel-2 reflectance (R^2 = 0.52–0.56). In the control scenario, both Sentinel-1 backscatter coefficients and Sentinel-2 band 12 (SWIR) reflectance featured a strong relationship with VSD (R^2 > 0.69). RF relative variable importance evaluated from the %IncMSE parameter followed the same pattern as the univariate relationships (Fig. 4), except in the case of Sentinel-2 band 4 (red) reflectance, which gained the greatest importance in the control plots.

External model validation based on the extrapolation of the RF predictive relationships from 1 to 2 years after wildfire featured an R^2 equal to 0.57 and an RMSE of 0.20 (Fig. 5), which involves a slight reduction in VSD predictive capacity with respect to the internal model validation (RMSE = 0.13).

All plant communities gradually recovered VSD over the postfire time series (Fig. 6). Nonetheless, 4 years after the fire disturbance, the VSD of each plant community was significantly lower than in the prefire scenario (p values <0.001) and, therefore, resilience has not been achieved at short term (Fig. 7 and Table S1). Plant communities dominated by resprouter species (i.e., heath shrublands and Pyrenean oak forests) featured significantly higher VSD recovery values (p values <0.001) at the end of the time series than communities dominated by facultative (gorse and broom shrublands) or obligate seeders (Scots pine) (Fig. 8 and Table S2).

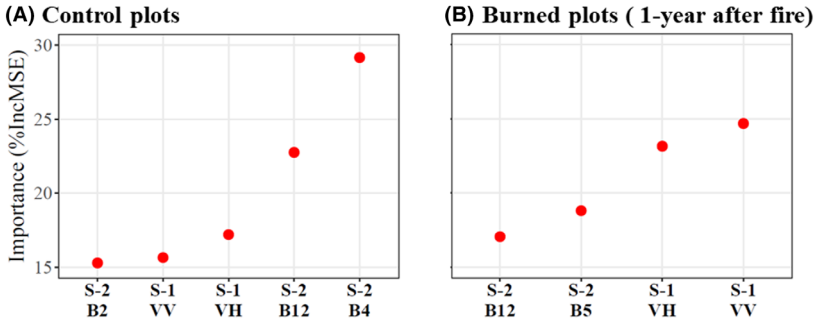

Figure 4. Relative variable importance in Random Forest models measured as the percentage increase in mean square error (%IncMSE), in unburned control plots (A) and burned plots 1 year after fire (B).

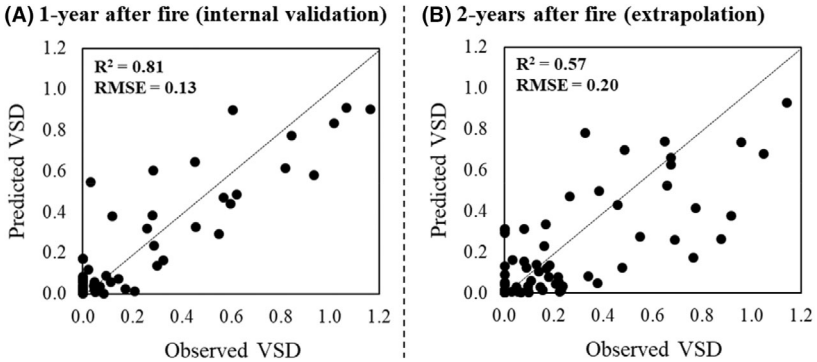

Figure 5. Relationship between observed and predicted vertical structure diversity index (VSD) 1 year after wildfire (internal model validation) and 2 years after wildfire (model extrapolation) through Random Forest models. The dotted black line represents the 1:1 line.

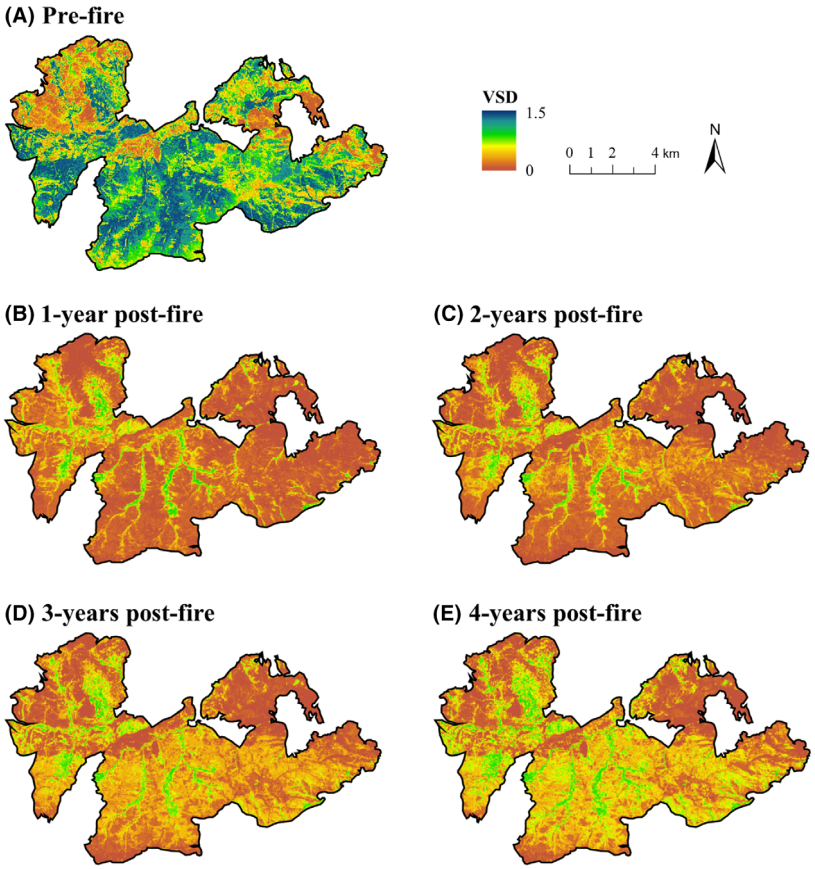

Figure 6. Maps of predicted vertical structure diversity index (VSD) by the Random Forest models throughout the pre- and postfire time series.

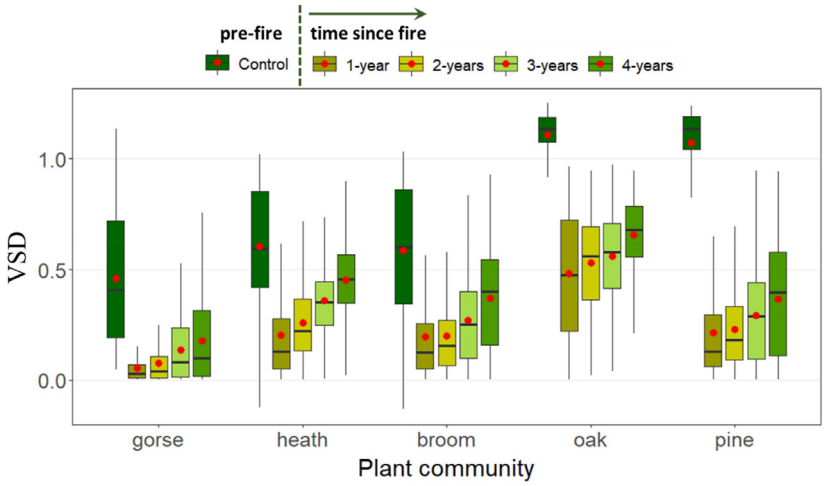

Figure 7. Boxplots showing the relationship between vertical structure diversity index and plant community type throughout the pre- and postfire time series.

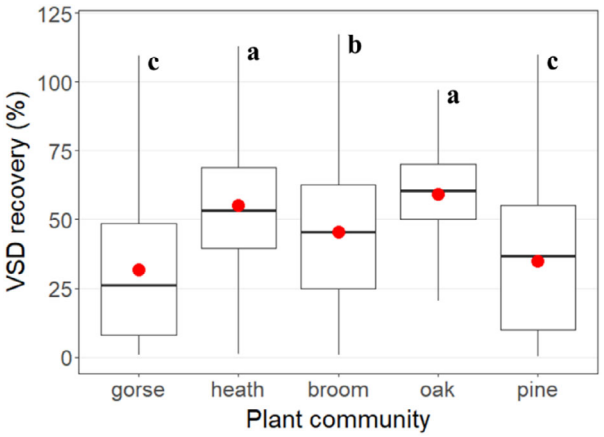

Figure 8. Boxplot showing the relationship between vertical structure diversity index recovery and plant community type. Lowercase letters denote significant differences in VSD recovery at the 0.05 level between plant communities (see Table S2).

Discussion

Prediction of vertical structure diversity by C-band SAR and optical data

Monitoring vegetation vertical structure diversity in fire-prone burned landscapes of the Mediterranean Basin is critical for implementing postfire management actions aimed at maintaining ecosystem function and processes affected by wildfire disturbance (Chergui et al., 2018; González-De Vega et al., 2016). The proposed remote sensing-based approach based on data fusion of Sentinel-1 SAR backscatter and Sentinel-2 reflectance successfully captured in this study the spatial variability in VSD through RF models in several pre- and postfire scenarios.

Sentinel-1 backscatter data in C-band featured a higher model contribution for characterizing VSD 1 year after fire than Sentinel-2 reflectance. In this sense, SAR signal in burned landscapes is more sensitive to changes in the forest structure than optical data (Tanase et al., 2015) because C-band SAR waves are directly influenced by the size distribution and density of stems, branches, and foliage (Bergen et al., 2009), particularly in Mediterranean forest and shrub plant communities (Belenguer-Plomer et al., 2019). In addition, fire consumption of leaves and small branches in the burned plots (i.e., reduced canopy closure) enables the penetration of SAR signal in shorter wavelengths to the lower vegetation strata (Tanase et al., 2010). The direct relationship between Sentinel-1 backscatter coefficient and VSD was consistent with previous research in which fire consumption reduced C-band backscatter intensity as a result of the reduction in the number of scatterers (i.e., lower VSD) throughout the vertical stand profile (e.g., Antikidis et al., 1998; Tanase et al., 2014). Conversely, Sentinel-2 reflectance bands gained the highest importance in the RF models of VSD in the unburned control plots, even though Sentinel-1 backscatter data were also selected as relevant in the model selection routine. The higher biomass density in unburned plots may prevent the penetration of C-band SAR signal to the forest floor compared with longer SAR wavelengths such as L-band data (Inoue et al., 2002; Jagdhuber, 2012; Tanase et al., 2010), undermining the strength of the relationship between SAR backscatter and VSD. In such scenarios, Sentinel-2 reflectance coupled with SAR backscatter may be associated with canopy architecture (Montesano et al., 2013) and top of canopy traits such as moisture content, shadowing, and photosynthetic capacity (Fernández-Guisuraga, Suárez-Seoane, & Calvo, 2021; Goetz & Dubayah, 2011; Healey et al., 2020), which are themselves proxies of subcanopy structural density (Conti et al., 2021; Gao et al., 2000). In fact, Sentinel-2 band 4 (red) and band 12 (SWIR) were selected in RF models as important variables because of their sensitivity to the above-mentioned traits (Fensholt & Sandholt, 2003; Karlson et al., 2015), which are generally enhanced in plant communities characterized by high structural complexity and lower red and SWIR reflectance values (Avitabile et al., 2012; Fernández-Guisuraga, Suárez-Seoane, et al., 2022). The latter explains the inverse relationship between VSD and the reflectance of Sentinel-2 bands.

Extrapolation of C-band SAR and optical predictive relationships of vertical structure diversity

Although the spatial and temporal transferability of remote sensing-based approaches is currently one of the biggest challenges in the field (Fernández-Guisuraga, Calvo, et al., 2019; Zandler et al., 2015), the extrapolation of the RF predictive relationships from 1 to 2 years after wildfire only entailed a reduction in the predictive capacity of the VSD from 0.13 to 0.20 in terms of RMSE. This behavior could be explained by the physical sense of SAR backscatter data for characterizing vegetation structure variability in burned areas (Kalogirou et al., 2014), which leads to an improvement in the transferability of predictive relationships (Fernández-Guisuraga, Verrelst, et al., 2021). The proposed SAR and optical synergistic approach could be transferable to other Mediterranean ecosystems and, in general, to biomes characterized by low to moderate vegetation biomass or high-intensity fire regimes in which biomass consumption enables the penetration of short wavelength SAR signal to the lower vegetation layers (Belenguer-Plomer et al., 2019). For

example, C-band SAR data have proven to be useful in the monitorization of stand structural characteristics in recently disturbed (i.e., early successional stages) North American boreal forests (Harrell et al., 1995; Ranson et al., 1997), characterized by high-intensity fire regime (van Leeuwen et al., 2014). In the tundra biome, which features typically low biomass values and where the role of wildfires in shaping ecosystem structure and dynamics has been underestimated Bartsch et al. (2020) and Jones et al. (2013) evidenced the ability of a Sentinel-1 and Sentinel-2 data fusion approach to retrieve tundra vegetation structural characteristics. Conversely, it is expected that backscatter saturation at short SAR wavelengths in biomes with high canopy closure and biomass, such as tropical forests (e.g., Englhart et al., 2011; Huang et al., 2018; Musthafa & Singh, 2022), do not allow to evaluate resilience to fire in terms of vegetation structural complexity through the proposed approach. Future research should consider the use of SAR sensors with longer wavelengths such as PALSAR-2 L-band SAR on-board ALOS-2 satellite (JAXA, 2022) or the P-band SAR instrument of the future Biomass mission (ESA, 2022e), which would penetrate the canopy to a higher extent in both unburned and postfire scenarios with strong vegetation responses (Kasischke et al., 2007; Tanase et al., 2010). Alternatively, the increased sensitivity of interferometric SAR (InSAR) or polarimetric InSAR to forest vertical structure (Garestier et al., 2008; Lu et al., 2016; Solberg et al., 2010) could provide promising advances in ecological studies of resilience to fire.

Resilience to fire in terms of vertical structure diversity recovery

Remote sensing estimates of VSD revealed that none of the plant communities dominated by shrub or tree species have recovered to a prefire state in the short term (4 years after fire disturbance), although their VSD values have increased progressively over the time series. Previous remote sensing research was conducted in similar Mediterranean plant communities in the western Mediterranean Basin (Fernández-Guisuraga et al., 2020; Fernández-Guisuraga, Suárez-Seoane, & Calvo, 2021) as well as chaparral shrublands in California (Kibler et al., 2019; Storey et al., 2016), evidenced that vegetation cover reached prefire conditions in the short-term after wildfire disturbance. These studies used fractional vegetation cover (FVC) as an engineering resilience indicator retrieved from passive optical data by means of vegetation indices, pixel unmixing models, and radiative transfer models. However, this indicator encompasses the recovery of the photosynthetic vegetation fraction seen from the nadir, regardless of the vegetation stratum in multilayered plant communities when dealing exclusively with optical data (Fernández-Guisuraga, Suárez-Seoane, & Calvo, 2021). Conversely, the recovery trends of the vertical complexity in the considered shrub and tree plant communities, identified through the fusion of active and passive remote sensing data, follow a slower progression as evidenced in the present study. The higher VSD recovery evidenced for heath shrublands and Pyrenean oak forests could be related to the remarkable resprouting ability of the dominant and accompanying species of both communities (Calvo et al., 2003), which enables fast recovery of plant aboveground biomass (Fernández-Guisuraga et al., 2020; Pausas & Keeley, 2014). In addition, lower fire intensities typically reached in Pyrenean oak forests (Calvo et al., 2003), also evidenced in previous research in the study site (Fernández-Guisuraga, Suárez-Seoane, García-Llamas, et al., 2021), favor tree survival and canopy re-establishment in the short-term (Tárrega et al., 1996).

Conclusion

The assessment of how the structural complexity of plant communities recovers to a predisturbance state is crucial for maintaining the ecosystem functioning in fire-prone landscapes and providing new insights about ecological resilience to fire. This study is a pioneer in the use of SAR and multispectral data fusion for this purpose. The physical sense and sensitivity of SAR signal to the size distribution and density of stems, branches and foliage, together with the strong association between multispectral reflectance and top-of-canopy traits and architecture, enabled accurate predictions of vertical structure diversity. Sentinel-1 backscatter data in C-band featured a higher contribution than Sentinel-2 reflectance in the modelization of vertical structure diversity in burned scenarios, with the opposite behavior occurring in unburned control areas. In addition, the proposed approach was transferable between different postfire scenarios. Despite the resprouting ability of the dominant species favoring a fast recovery of plant aboveground biomass and vertical structure diversity recovery, neither plant community reached a prefire state regarding this ecological resilience indicator.

Acknowledgments

This study was financially supported by the Spanish Ministry of Economy and Competitiveness, and the European Regional Development Fund (ERDF), in the framework of the FIRESEVES (AGL2017-86075-C2-1-R) project, and by the Regional Government of Castilla and León in the framework of the WUIFIRECYL (LE005P20) project.

References

AEMET. (2022) *Agencia Estatal de Meteorología*. Madrid: AEMET Open Data. Available at: http://www.aemet.es/es/datos_abiertos/AEMET_OpenData [Accessed 3rd February 2022].

Angelo, J.J. (2010) *Characterizing the vertical structure and structural diversity of Florida Oak scrub vegetation using discrete-return LiDAR*. Thesis Dissertation. USA: University of Central Florida.

Antikidis, E., Arino, O., Arnaud, A. & Laur, H. (1998) ERS SAR coherence & ATSR hot spots: a synergy for mapping deforested areas. The special case of the 1997 fire event in Indonesia. *European Space Agency Publication*, **441**, 355–360.

Avitabile, V., Baccini, A., Friedl, M.A. & Schmullius, C. (2012) Capabilities and limitations of Landsat and land cover data for aboveground woody biomass estimation of Uganda. *Remote Sensing of Environment*, **117**, 366–380.

Bartsch, A., Widhalm, B., Leibman, M., Ermokhina, K., Kumpula, T., Skarin, A. et al. (2020) Feasibility of tundra vegetation height retrieval from Sentinel-1 and Sentinel-2 data. *Remote Sensing of Environment*, **237**, 111515.

Belenguer-Plomer, M.A., Tanase, M.A., Fernandez-Carrillo, A. & Chuvieco, E. (2019) Burned area detection and mapping using Sentinel-1 backscatter coefficient and thermal anomalies. *Remote Sensing of Environment*, **233**, 111345.

Bergen, K.M., Goetz, S.J., Dubayah, R.O., Henebry, G.M., Hunsaker, C.T., Imhoff, M.L. et al. (2009) Remote sensing of vegetation 3-D structure for biodiversity and habitat: review and implications for lidar and radar spaceborne missions. *Journal of Geophysical Research*, **114**, G00E06.

Bivand, R., Keitt, T. & Rowlingson, B. (2021) rgdal: Bindings for the 'Geospatial' Data Abstraction Library R package version. pp. 15–23. Available from: https://CRANR-projectorg/package=rgdal

Breiman, L. (2001) Random forests. *Machine Learning*, **45**, 5–32.

Calvo, L., Santalla, S., Marcos, E., Valbuena, L., Tárrega, R. & Luis, E. (2003) Regeneration after wildfire in communities dominated by *Pinus pinaster*, an obligate seeder, and in others dominated by *Quercus pyrenaica*, a typical resprouter. *Forest Ecology and Management*, **184**, 209–223.

Calvo, L., Santalla, S., Valbuena, L., Marcos, E., Tárrega, R. & Luis-Calabuig, E. (2008) Post-fire natural regeneration of a *Pinus pinaster* forest in NW Spain. *Plant Ecology*, **197**, 81–90.

Casenave, J.L., Pelotto, J.P. & Protomastro, J. (1995) Edge-interior differences in vegetation structure and composition in a Chaco semi-arid forest, Argentina. *Forest Ecology and Management*, **72**, 61–69.

Chergui, B., Fahd, S. & Santos, X. (2018) Quercus suber forest and Pinus plantations show different post-fire resilience in Mediterranean north-western Africa. *Annals of Forest Science*, **75**, 64.

Conti, L., Malavasi, M., Galland, T., Komárek, J., Lagner, O., Carmona, C.P. et al. (2021) The relationship between species and spectral diversity in grassland communities is mediated by their vertical complexity. *Applied Vegetation Science*, **24**, e12600.

Cuevas-González, M., Gerard, F., Baltzer, H. & Riaño, D. (2009) Analysing forest recovery after wildfire disturbance in boreal Siberia using remotely sensed vegetation indices. *Global Change Biology*, **15**, 561–577.

Cutler, D.R., Edwards, T.C., Beard, K.H., Cutler, A., Hess, K.T., Gibson, J. et al. (2007) Random forests for classification in ecology. *Ecology*, **88**, 2783–2792.

Delamater, P.L., Messina, J.P., Mark, J.K. & Cochrane, A. (2012) A hybrid visual estimation method for the collection of ground truth fractional coverage data in a humid tropical environment. *International Journal of Applied Earth Observation and Geoinformation*, **18**, 504–514.

Díaz-Delgado, R., Lloret, F., Pons, X. & Terradas, J. (2002) Satellite evidence of decreasing resilience in Mediterranean plant communities after recurrent wildfires. *Ecology*, **83**, 2293–2303.

Doblas-Miranda, E., Alonso, R., Arnan, X., Bermejo, V., Brotons, L., de las Heras, J. et al. (2017) A review of the combination among global change factors in forests, shrublands and pastures of the Mediterranean Region: beyond drought effects. *Global and Planetary Change*, **148**, 42–54.

Drever, C.R., Peterson, G., Messier, C., Bergeron, Y. & Flannigan, M. (2006) Can forest management based on natural disturbances maintain ecological resilience? *Canadian Journal of Forest Research*, **36**, 2285–2299.

Englhart, S., Keuck, V. & Siegert, F. (2011) Aboveground biomass retrieval in tropical forests - the potential of combined X- and L-band SAR data use. *Remote Sensing of Environment*, **115**, 1260–1271.

ESA. (2022a) Sentinel-1 SAR User Guide. Available at: https://sentinels.copernicus.eu/web/sentinel/user-guides/sentinel-1-sar [Accessed 25 March 2022].

ESA. (2022b) Sentinel-1 mission. Available at: https://sentinel.esa.int/web/sentinel/missions/sentinel-1 [Accessed 25 March 2022].

ESA. (2022c) Sentinel Application Platform (SNAP). Available at: https://earth.esa.int/eogateway/tools/snap [Accessed 25 March 2022].

ESA. (2022d) Sentinel-2 MSI User Guide. Available at: https://sentinel.esa.int/web/sentinel/user-guides/sentinel-2-msi. [Accessed 25 March 2022].

ESA. (2022e) Biomass mission overview. Available at: https://earth.esa.int/eogateway/missions/biomass/description [Accessed 05 April 2022].

Fensholt, R. & Sandholt, I. (2003) Derivation of a shortwave infrared water stress index from MODIS near- and shortwave infrared data in a semiarid environment. *Remote Sensing of Environment*, **87**, 111–121.

Fernández-García, V., Beltrán-Marcos, D., Fernández-Guisuraga, J.M., Marcos, E. & Calvo, L. (2022) Predicting potential wildfire severity across Southern Europe with global data sources. *Science of the Total Environment*, **829**, 154729.

Fernández-Guisuraga, J.M., Suárez-Seoane, S. & Calvo, L. (2019) Modeling *Pinus pinaster* forest structure after a large wildfire using remote sensing data at high spatial resolution. *Forest Ecology and Management*, **446**, 257–271.

Fernández-Guisuraga, J.M., Calvo, L., Fernández-García, V., Marcos-Porras, E., Taboada, A. & Suárez-Seoane, S. (2019) Efficiency of remote sensing tools for post-fire management along a climatic gradient. *Forest Ecology and Management*, **433**, 553–562.

Fernández-Guisuraga, J.M., Calvo, L. & Suárez-Seoane, S. (2020) Comparison of pixel unmixing models in the evaluation of post-fire forest resilience based on temporal series of satellite imagery at moderate and very high spatial resolution. *ISPRS Journal of Photogrammetry and Remote Sensing*, **164**, 217–228.

Fernández-Guisuraga, J.M., Suárez-Seoane, S. & Calvo, L. (2021) Radiative transfer modeling to measure fire impact and forest engineering resilience at short-term. *ISPRS Journal of Photogrammetry and Remote Sensing*, **176**, 30–41.

Fernández-Guisuraga, J.M., Verrelst, J., Calvo, L. & Suárez-Seoane, S. (2021) Hybrid inversion of radiative transfer models based on high spatial resolution satellite reflectance data improves fractional vegetation cover retrieval in heterogeneous ecological systems after fire. *Remote Sensing of Environment*, **255C**, 112304.

Fernández-Guisuraga, J.M., Suárez-Seoane, S., García-Llamas, P. & Calvo, L. (2021) Vegetation structure parameters determine high burn severity likelihood in different ecosystem types: a case study in a burned Mediterranean landscape. *Journal of Environmental Management*, **288**, 112462.

Fernández-Guisuraga, J.M., Suárez-Seoane, S., Fernandes, P.M., Fernández-García, V., Fernández-Manso, A., Quintano, C. et al. (2022) Pre-fire aboveground biomass, estimated from LiDAR, spectral and field inventory data, as a major driver of burn severity in maritime pine (*Pinus pinaster*) ecosystems. *Forest Ecosystems*, **9**, 100022.

Fernández-Guisuraga, J.M., Calvo, L., Fernandes, P.M. & Suárez-Seoane, S. (2022) Short-term recovery of the aboveground carbon stock in Iberian Shrublands at the extremes of an environmental gradient and as a function of burn severity. *Forests*, **13**, 145.

Fernandez-Manso, A., Quintano, C. & Roberts, D.A. (2016) Burn severity influence on post-fire vegetation cover resilience from Landsat MESMA fraction images time series in Mediterranean forest ecosystems. *Remote Sensing of Environment*, **184**, 112–123.

Folke, C. (2006) Resilience: the emergence of a perspective for social–ecological systems analysis. *Global Environmental Change*, **16**, 253–267.

Freemark, K.E. & Merriam, H.G. (1986) Importance of area and habitat heterogeneity to bird assemblages in temperate forest fragments. *Biological Conservation*, **36**, 115–141.

Gao, X., Huete, A.R., Ni, W. & Miura, T. (2000) Optical–biophysical relationships of vegetation spectra without background contamination. *Remote Sensing of Environment*, **74**, 609–620.

Gara, T.W., Darvishzadeh, R., Skidmore, A.K. & Wang, T. (2018) Impact of vertical canopy position on leaf spectral properties and traits across multiple species. *Remote Sensing*, **10**, 346.

García-Llamas, P., Suárez-Seoane, S., Fernández-Guisuraga, J.M., Fernández-García, V., Fernández-Manso, A., Quintano, C. et al. (2019) Evaluation and comparison of Landsat 8, Sentinel-2 and Deimos-1 remote sensing indices for assessing burn severity in Mediterranean fire-prone ecosystems. *International Journal of Applied Earth Observation and Geoinformation*, **80**, 137–144.

García-Llamas, P., Suárez-Seoane, S., Fernández-Manso, A., Quintano, C. & Calvo, L. (2020) Evaluation of fire severity in fire prone-ecosystems of Spain under two different environmental conditions. *Journal of Environmental Management*, **271**, 110706.

Garestier, F., Dubois-Fernandez, P.C. & Papathanassiou, K.P. (2008) Pine forest height inversion using single-pass X-band PolInSAR data. *IEEE Transactions on Geoscience and Remote Sensing*, **46**, 59–68.

GEODE. (2022) Mapa Geológico Digital continuo de España. Available at: http://mapas.igme.es/gis/services/Cartografia_Geologica/IGME_Geode_50/MapServer/WMSServer/ [Accessed 24 March 2022].

Goetz, S. & Dubayah, R. (2011) Advances in remote sensing technology and implications for measuring and monitoring forest carbon stocks and change. *Carbon Management*, **2**, 231–244.

González-De Vega, S., De las Heras, J. & Moya, D. (2016) Resilience of Mediterranean terrestrial ecosystems and fire severity in semiarid areas: responses of Aleppo pine forests in the short, mid and long term. *Science of the Total Environment*, **573**, 1171–1177.

Gough, C.M., Atkins, J.W., Fahey, R.T. & Hardiman, B.S. (2019) High rates of primary production in structurally complex forests. *Ecology*, **100**, e02864.

Gunderson, L.H. & Holling, C.S. (2002) *Panarchy: understanding transformations in human and natural systems*. Washington, DC: Island Press.

Harrell, P.A., Bourgeau-Chavez, L.L., Kasischke, E.S., French, N.H.F. & Christensen, N.L. (1995) Sensitivity of ERS-1 and JERS-1 radar data to biomass and stand structure in Alaskan boreal forest. *Remote Sensing of Environment*, **54**, 247–260.

Healey, S.P., Yang, Z., Gorelick, N. & Ilyushchenko, S. (2020) Highly local model calibration with a new GEDI LiDAR asset on google earth engine reduces landsat forest height signal saturation. *Remote Sensing*, **12**, 2840.

Hijmans, R.J. (2021) raster: Geographic Data Analysis and Modeling R package version. pp. 34–10. Available at: https://CRANR-projectorg/package=raster

Huang, C., Ye, Z., Deng, C., Zhang, Z. & Wan, Z. (2016) Mapping Above-Ground Biomass by Integrating optical and SAR imagery: a case study of Xixi National Wetland Park, China. *Remote Sensing*, **8**, 1–19.

Huang, X., Ziniti, B., Torbick, N. & Ducey, M.J. (2018) Assessment of forest above ground biomass estimation using multi-temporal C-band Sentinel-1 and polarimetric L-band PALSAR-2 data. *Remote Sensing*, **10**, 1424.

Inoue, A., Kurosu, T., Maeno, H., Uratsuka, S., Kozu, T., Dabrowska-Zielinska, K. et al. (2002) Season-long daily measurements of multifrequency (Ka, Ku, X, C, and L) and full-polarization backscatter signatures over paddy rice field and their relationship with biological variables. *Remote Sensing of Environment*, **81**, 194–204.

Ireland, G. & Petropoulos, G.P. (2015) Exploring the relationships between post-fire vegetation regeneration dynamics, topography and burn severity: a case study from the Montane Cordillera Ecozones of Western Canada. *Applied Geography*, **56**, 232–248.

Jagdhuber, T. (2012) *Soil parameter retrieval under vegetation cover using SAR polarimetry*. Thesis Dissertation. Germany: University of Potsdam.

JAXA. (2022) ALOS-2 Project/PALSAR-2. Availablet at: https://www.eorc.jaxa.jp/ALOS-2/en/about/palsar2.htm. [Accessed 05 April 2022].

Jia, K., Liang, S., Gu, X., Baret, F., Wei, X., Wang, X. et al. (2016) Fractional vegetation cover estimation algorithm for Chinese GF-1 wide field view data. *Remote Sensing of Environment*, **177**, 184–191.

Jin, Y., Randerson, J.T., Goetz, S.J., Beck, P.S.A., Loranty, M.M. & Goulden, M.L. (2012) The influence of burn severity on postfire vegetation recovery and albedo change during early succession in North American boreal forests. *Journal of Geophysical Research*, **117**, G01036.

Johnstone, J.F., Allen, C.D., Franklin, J.F., Frelich, L.E., Harvey, B.J., Higuera, P.E. et al. (2016) Changing disturbance regimes, ecological memory, and forest resilience. *Frontiers in Ecology and Environment*, **14**, 369–378.

Jones, B.M., Breen, A.L., Gaglioti, B.V., Mann, D.H., Rocha, A.V., Grosse, G. et al. (2013) Identification of unrecognized tundra fire events on the north slope of Alaska. *Journal of Geophysical Research Biogeosciences*, **118**, 1334–1344.

Kalogirou, V., Ferrazzoli, P., Vecchia, A.D. & Foumelis, M. (2014) On the SAR backscatter of burned forests: a model-based study in C-band, over burned pine canopies. *IEEE Transactions on Geoscience and Remote Sensing*, **52**, 6205–6215.

Karlson, M., Ostwald, M., Reese, H., Sanou, J., Tankoano, B. & Mattsson, E. (2015) Mapping tree canopy cover and aboveground biomass in Sudano-Sahelian woodlands using Landsat 8 and random forest. *Remote Sensing*, **7**, 10017–10041.

Kassambara, A. (2021) rstatix: Pipe-Friendly Framework for Basic Statistical Tests. R package version 0.7.0. Available from: https://CRAN.R-project.org/package=rstatix.

Kasischke, E.S., Bourgeau-Chavez, L.L. & Johnstone, J.F. (2007) Assessing spatial and temporal variations in surface soil moisture in fire-disturbed black spruce forests in Interior Alaska using spaceborne synthetic aperture radar imagery - implications for post-fire tree recruitment. *Remote Sensing of Environment*, **108**, 42–58.

Kibler, C.L., Parkinson, A.-M.L., Peterson, S.H., Roberts, D.A., D'Antonio, C.M., Meerdink, S.K. et al. (2019) Monitoring post-fire recovery of chaparral and conifer species using field surveys and landsat time series. *Remote Sensing*, **11**, 2963.

Kuhn, M. (2020) caret: Classification and Regression Training R package version. pp. 60–86. Available from: https://CRANR-projectorg/package=caret

LaRue, E.A., Hardiman, B.S., Elliott, J.M. & Fei, S. (2019) Structural diversity as a predictor of ecosystem function. *Environmental Research Letters*, **14**, 114011.

Liaw, A. & Wiener, M. (2002) Classification and regression by RandomForest. *R News*, **2**, 18–22.

Lu, D., Chen, Q., Wang, G., Liu, L., Li, G. & Moran, E. (2016) A survey of remote sensing-based aboveground biomass estimation methods in forest ecosystems. *International Journal of Digital Earth*, **9**, 63–105.

MacArthur, R.H. & MacArthur, J.W. (1961) On bird species diversity. *Ecology*, **42**, 595–599.

Meng, R., Wu, J., Zhao, F., Cook, B.D., Hanavan, R.P. & Serbin, S.P. (2018) Measuring short-term post-fire forest recovery across a burn severity gradient in a mixed pine-oak forest using multi-sensor remote sensing techniques. *Remote Sensing of Environment*, **210**, 282–296.

Meeussen, C., Govaert, S., Vanneste, T., Calders, K., Bollmann, K., Brunet, J. et al. (2020) Structural variation of forest edges across Europe. *Forest Ecology and Management*, **462**, 117929.

Minchella, A., Del Frate, F., Capogna, F., Anselmi, S. & Manes, F. (2009) Use of multitemporal SAR data for monitoring vegetation recovery of Mediterranean burned areas. *Remote Sensing of Environment*, **113**, 588–597.

Montes, F., Sánchez, M., del Río, M. & Cañellas, I. (2005) Using historic management records to characterize the effects of management on the structural diversity of forests. *Forest Ecology and Management*, **207**, 279–293.

Montesano, P.M., Cook, B.D., Sun, G., Simard, M., Nelson, R.F., Ranson, K.J. et al. (2013) Achieving accuracy requirements for forest biomass mapping: a spaceborne data fusion method for estimating forest biomass and LiDAR sampling error. *Remote Sensing of Environment*, **130**, 153–170.

Müller, F., Bergmann, M., Dannowski, R., Dippner, J.W., Gnauck, A., Haase, P. et al. (2016) Assessing resilience in

long-term ecological data sets. *Ecological Indicators*, **65**, 10–43.

Musthafa, M. & Singh, G. (2022) Improving forest above-ground biomass retrieval using multi-sensor L- and C- band SAR data and multi-temporal spaceborne LiDAR data. *Frontiers in Forest and Global Change*, **10**, 822704.

Naidoo, L., van Deventer, H., Ramoelo, A., Mathieu, R., Nondlazi, B. & Gangat, R. (2019) Estimating above ground biomass as an indicator of carbon storage in vegetated wetlands of the grassland biome of South Africa. *International Journal of Applied Earth Observation and Geoinformation*, **78**, 118–129.

Newton, A.C. & Cantarello, E. (2015) Restoration of forest resilience: an achievable goal? *New Forests*, **46**, 645–668.

Ninyerola, M., Pons, X., Roure, J.M., 2005. *Atlas Climático Digital de la Península Ibérica. Metodología y aplicaciones en bioclimatología y geobotánica*. Barcelona: Universidad Autónoma de Barcelona.

Patenaude, G., Milne, R. & Dawson, T.P. (2005) Synthesis of remote sensing approaches for forest carbon estimation: reporting to the Kyoto Protocol. *Environmental Science & Policy*, **8**, 161–178.

Pausas, J.G., Llovet, J., Rodrigo, A. & Vallejo, R. (2008) Are wildfires a disaster in the Mediterranean basin? A review. *International Journal of Wildland Fire*, **17**, 713–723.

Pausas, J.G. & Keeley, J.E. (2014) Evolutionary ecology of resprouting and seeding in fire-prone ecosystems. *New Phytologist*, **204**, 55–65.

Picotte, J.J. & Robertson, K.M. (2011) Validation of remote sensing of burn severity in south-eastern US ecosystems. *International Journal of Wildland Fire*, **20**, 453–464.

Probst, P. & Boulesteix, A.L. (2018) To tune or not to tune the number of trees in Random Forest. *Journal of Machine Learning Research*, **18**, 1–18.

R Core Team (2021). *R: a language and environment for statistical computing*. Vienna, Austria: R Foundation for Statistical Computing. Available from: https://www.R-project.org/.

Ranson, K.J., Sun, G., Lang, R.H., Chauhan, N.S., Cacciola, R.J. & Kilic, O. (1997) Mapping of boreal forest biomass from spaceborne synthetic aperture radar. *Journal of Geophysical Research*, **102**, 29599–29610.

Rivas-Martínez, S., Rivas-Sáenz, S. & Penas, A. (2011) Worldwide bioclimatic classification system. *Global Geobotany*, **1**, 1–634.

Sagra, J., Moya, D., Plaza-Álvarez, P.A., Lucas-Borja, M.E., González-Romero, J., De las Heras, J. et al. (2019) Prescribed fire effects on early recruitment of Mediterranean pine species depend on fire exposure and seed provenance. *Forest Ecology and Management*, **441**, 253–261.

San-Miguel-Ayanz, J., Rodrigues, M., de Oliveira, S.S., Pacheco, C.K., Moreira, F., Duguy, B., Camia, A., 2012. Land cover change and fire regime in the European Mediterranean region. In: Moreira, F., Arianoustsou, M., Corona, P., de las Heras, J. (Eds.), *Post-fire management and restoration of southern European forests - managing forest ecosystems*, Vol. **24**. New York: Springer, pp. 21–43.

Santana, J., Porto, M., Reino, L. & Beja, P. (2011) Long-term understory recovery after mechanical fuel reduction in Mediterranean cork oak forests. *Forest Ecology and Management*, **261**, 447–459.

Seidl, R., Rammer, W. & Spies, T.A. (2014) Disturbance legacies increase the resilience of forest ecosystem structure, composition, and functioning. *Ecological Applications*, **24**, 2063–2077.

Small, D. & Schubert, A. (2008) Guide to ASAR Geocoding, RSL-ASAR-GC-AD, Issue 1.0.

Small, D. (2011) Flattening gamma: radiometric terrain correction for SAR imagery. *IEEE Transactions on Geoscience and Remote Sensing*, **49**, 3081–3093.

Solberg, S., Astrup, R., Gobakken, T., Næsset, E. & Weydahl, D.J. (2010) Estimating spruce and pine biomass with interferometric X-band SAR. *Remote Sensing of Environment*, **114**, 2353–2360.

Staudhammer, C.L. & LeMay, V.M. (2001) Introduction and evaluation of possible indices of stand structural diversity. *Canadian Journal of Forest Research*, **31**, 1105–1115.

Storey, E.A., Stow, D.A. & O'Leary, J.F. (2016) Assessing postfire recovery of chamise chaparral using multi-temporal spectral vegetation index trajectories derived from Landsat imagery. *Remote Sensing of Environment*, **183**, 53–64.

Strahler, A.H. (1980) The use of prior probabilities in maximum likelihood classification of remotely sensed data. *Remote Sensing of Environment*, **10**, 135–163.

Suárez-Seoane, S., Osborne, P.E. & Baudry, J. (2002) Responses of birds of different biogeographic origins and habitat requirements to agricultural land abandonment in northern Spain. *Biological Conservation*, **105**, 333–344.

Tanase, M.A., Santoro, M., de la Riva, J., Pérez-Cabello, F. & Le Toan, T. (2010) Sensitivity of X-, C-, and L-band SAR backscatter to burn severity in mediterranean pine forests. *IEEE Transactions on Geoscience and Remote Sensing*, **48**, 3663–3675.

Tanase, M.A., Santoro, M., Aponte, C. & de la Riva, J. (2014) Polarimetric properties of burned forest areas at C- and L-band. *IEEE Journal of Selected Topics in Applied Earth Observation and Remote Sensing*, **7**, 267–276.

Tanase, M.A., Kennedy, R. & Aponte, C. (2015) Radar Burn Ratio for fire severity estimation at canopy level: an example for temperate forests. *Remote Sensing of Environment*, **170**, 14–31.

Tárrega, R., Luis-Calabuig, E. & Marcos, E. (1996) Relationship between soil changes and plant succession in postfire regeneration of Quercus pyrenaica ecosystems. *Arid Soil Research and Rehabilitation*, **10**, 85–93.

van Leeuwen, T.T., van der Werf, G.R., Hoffmann, A.A., Detmers, R.G., Rücker, G., French, N.H.F. et al. (2014)

Biomass burning fuel consumption rates: a field measurement database. *Biogeosciences*, **11**, 7305–7329.
Veraverbeke, S., Gitas, I., Katagis, T., Polychronaki, A., Somers, B. & Goossens, R. (2012) Assessing post-fire vegetation recovery using red–near infrared vegetation indices: accounting for background and vegetation variability. *ISPRS Journal of Photogrammetry and Remote Sensing*, **68**, 28–39.
Vieira, J., Campelo, F. & Nabais, C. (2010) Intra-annual density fluctuations of *Pinus pinaster* are a record of climatic changes in the western Mediterranean region. *Canadian Journal of Forest Research*, **40**, 1567–1575.
Vila, G. & Barbosa, P. (2010) Post-fire vegetation regrowth detection in the Deiva Marina region (Liguria-Italy) using Landsat TM and ETM+ data. *Ecological Modelling*, **221**, 75–84.
Wang, J., Xiao, X., Bajgain, R., Starks, P., Steiner, J., Doughty, R.B. et al. (2019) Estimating leaf area index and aboveground biomass of grazing pastures using Sentinel-1, Sentinel-2 and Landsat images. *ISPRS Journal of Photogrammetry and Remote Sensing*, **154**, 189–201.
Wiens, J.A. & Rotenberry, J.T. (1981) Habitat associations and community structure of birds in shrubsteppe environments. *Ecological Monographs*, **51**, 21–42.
Williams, S. & Marsh, H. (1998) Changes in small mammal assemblage structure across a rain forest/open forest ecotone. *Journal of Tropical Ecology*, **14**, 187–198.
Wood, E.M., Pidgeon, A.M., Radeloff, V.C. & Keuler, N.S. (2012) Image texture as a remotely sensed measure of vegetation structure. *Remote Sensing of Environment*, **121**, 516–526.
Zandler, H., Brenning, A. & Samimi, C. (2015) Potential of space-borne hyperspectral data for biomass quantification in an arid environment: advantages and limitations. *Remote Sensing*, **7**, 4565–4580.
Zhao, F.R., Meng, R., Huang, C., Zhao, M., Zhao, F.A., Gong, P. et al. (2016) Long-term post-disturbance forest recovery in the greater yellowstone ecosystem analyzed using landsat time series stack. *Remote Sensing*, **8**, 898.

Supporting Information

Additional supporting information may be found online in the Supporting Information section at the end of the article.

Table S1 One-way repeated measures ANOVA and Tukey's HSD test results for determining the earliest point in the postfire time series where vertical structure diversity (VSD) does not differ significantly from prefire VSD.

Table S2. One-way ANOVA and Tukey's HSD test results for evaluating vertical structure diversity recovery differences between plant communities.

